IEEE Access
Multidisciplinary ⋮ Rapid Review ⋮ Open Access Journal

Received 13 May 2024, accepted 17 June 2024, date of publication 2 July 2024, date of current version 12 July 2024.

Digital Object Identifier 10.1109/ACCESS.2024.3422291

RESEARCH ARTICLE

A Merging Strategy Framework for Connected and Automated Vehicles in Multi-Lane Mixed Traffic Scenarios

YE LI[1], YUNYU ZHANG[2], AND YINGYUE MA[1]
[1]School of Traffic and Transportation Engineering, Central South University, Changsha, Hunan 410075, China
[2]School of Traffic and Transportation, Beijing Jiaotong University, Beijing 100044, China

Corresponding author: Yingyue Ma (yingyue@csu.edu.cn)

This work was supported in part by the Advanced Multidisciplinary Project of Central South University (No. 2023QYJC016).

ABSTRACT Frequent merging, overtaking, and lane-changing behaviors at freeway on-ramp areas usually cause traffic bottlenecks with low efficiency and significant safety concerns. Fortunately, the development of connected and autonomous vehicles (CAVs) presents a promising technology for improving merging efficiency and safety. Current research on CAV merging strategies mainly focuses on single-lane scenarios and relies heavily on oversimplified simulation tests. To this end, this study proposes a merging strategy framework for the merging CAV in complex multi-lane mixed traffic scenarios, taking into account the potential interference caused by other vehicles' lane-changing behaviors. First, a merging gap selection method assists the merging CAV in choosing a more suitable merging gap. Then, a lateral speed control strategy provides the CAV with highly efficient lateral guidance by giving optimal lateral speed control parameters. Furthermore, a pre-merging safety preparation method controls the CAV to adjust its speed longitudinally to avoid potential conflicts. Finally, the merging execution part is proposed to guarantee the CAV an effective, safe, and comfortable merging experience. The proposed model is tested in merging scenarios extracted from the Delft freeway trajectory dataset. Results indicate that the proposed merging strategy can significantly improve the merging efficiency by 45%, while offering a safe and comfortable merging trajectory for CAVs in multi-lane mixed traffic scenarios.

INDEX TERMS Freeway, multi-lane, merge, CAV, trajectory optimization.

I. INTRODUCTION

Freeways are designed to offer drivers an efficient, comfortable, and economical driving environment. However, the on-ramp areas often become bottlenecks in freeways due to frequent speed-changing and lane-changing behaviors, making them crucial areas for solving traffic congestion and traffic accidents [1], [2], [3]. Owing to the frequent disturbances caused by vehicles merging from on-ramps, coupled with unpredictable lane-changing and overtaking maneuvers on the mainline [4]. Improving the efficiency and safety of on-ramps remains a persistent challenge.

With the advancement of automation and communication technologies, connected and autonomous vehicles (CAVs) are emerging as a promising direction for the future of transportation, holding substantial potential to improve both traffic efficiency and safety [5], [6], [7]. Leveraging advanced communication and automation technologies, CAVs can sense and exchange information with the surrounding vehicles, empowering them to formulate optimal driving strategies and achieve precise control. As a result, they could offer a new solution to mitigate traffic congestion and reduce accidents on freeway on-ramps.

Many researchers have proposed merging strategies for CAVs, which can be categorized into two groups according to the application scenarios: complete CAV environment and mixed traffic environment. Considering the complete

The associate editor coordinating the review of this manuscript and approving it for publication was Razi Iqbal.

CAV environment, some research focuses on the higher-level control for the merging sequence. For example, some divided all vehicles into multiple groups or platoons based on their initial positions and then formulated the best merging sequence [8], [9], [10], [11]. Some studies also concentrate on the lower level of control for vehicles' trajectories to optimize the merging efficiency. For instance, Cao et al. [12] developed cooperative merging trajectories by controlling the mainline vehicles to create a larger gap. Rios-Torres and Malikopoulos [13] proposed an optimization framework based on a first-in-first-out queue and an analytical closed-form solution, obtaining an optimal trajectory that reduces fuel consumption. Similarly, Ntousakis et al. [14] and Letter and Elefteriadou [15] developed a longitudinal control model in which merging vehicles can generate their optimal trajectory based on the information of their leaders. Further, several researchers focus on a two-level hierarchical control framework. Tang et al. [16] proposed a two-level programming model, which determines the merging sequence through mixed integer programming at a high level and the merging trajectories of CAVs at a low level. Fukuyama [17] employed a game-theory-based approach to determine both the optimal merging sequence and trajectories, which is realized by the interactions between a competing pair of vehicles. Although merging behaviors in the complete CAV environment have been explored in the above studies, it is also crucial to consider mixed traffic scenarios, particularly at a low penetration rate of CAVs.

In mixed traffic flow conditions, Pueboobpaphan et al. [18] proposed a decentralized merging assistant to facilitate traffic flow stability by controlling the mainline vehicles to create gaps for ramp vehicles. Rios-Torres and Malikopoulos [19] explored the influence of different penetration rates of CAVs on the energy consumption at merging tasks. Zhou et al. [20] developed a motion planning strategy for both a ramp merging vehicle and a mainline facilitating vehicle. Based on this, Zhou et al. [21] further introduced a lower bound on the cooperative speed of the facilitating vehicle to mitigate the impact of a facilitating maneuver on following traffic. Karimi et al. [22] modeled six mixed traffic scenarios composed of vehicle triplets (the merging vehicle, its leader, and its follower), which are defined based on various combinations of CAVs and human-driven vehicles.

According to the above literature review, previous studies mainly focus on merging behaviors at the freeway segment consisting of one single main lane and an on-ramp. However, the lane-changing behaviors of vehicles on other main lanes may also influence on-ramp vehicles' merging, which is only taken into account by a few studies. Karbalaieali et al. [23] considered a two-lane highway scenario where the merging vehicles chose to merge either ahead of, behind, or within a platoon, based on a cost function. Zhu et al. [24] proposed a cooperative merging strategy that enhances efficiency by creating gaps on main lanes and formulating queues on the on-ramp. However, these studies are always based on the assumption that all vehicles are CAVs or make simple assumptions on the driving patterns of HDVs, which simplifies the complexity of multi-lane scenarios and mixed traffic flow.

To address these research gaps, this study aims to propose a merging strategy framework for CAVs in multi-lane mixed traffic flow scenarios, with the following contributions:

(1) A multi-stage merging strategy framework is established for CAVs in the mixed traffic flow, including lateral speed control, merging gap selection, and a two-stage merging operation (pre-merging safety preparation and merging execution).

(2) The influence of mainline vehicles on merging CAVs in a multi-lane scenario (two main lanes and one on-ramp) is taken into account by the proposed model.

(3) The model aims to enhance merging efficiency while ensuring safety for the merging CAV and has been validated with real merging scenario data.

The remainder of this manuscript is organized as follows. Section II presents the multi-stage merging strategy framework. Section III describes the numerical experiment. The model solution results are analyzed in Section IV. Section V summarizes the conclusions.

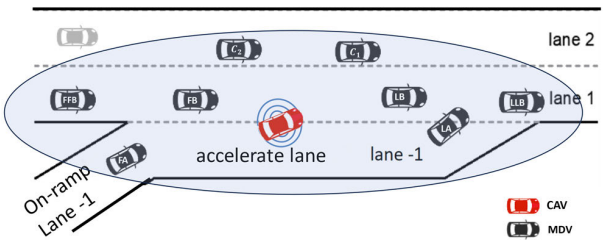

FIGURE 1. The schematic diagram of the merging vehicle group.

II. METHODOLOGY

As Fig. 1 shows, a typical complex multi-lane merging scenario includes an on-ramp, an acceleration lane, and two main lanes nearby. Such multi-lane configurations often prompt lane-changing and overtaking behaviors among vehicles. For example, vehicles traveling in Lane 2 may transition to Lane 1, thereby influencing the merging gap available to the merging vehicle. To more precisely clarify the scope of our research, the concept of "merging vehicle group" is defined, which may consist of the merging vehicle and its surrounding vehicles. Note that the relative positions of vehicles in the "merging vehicle group" are dynamically changing during the whole merging process.

Given the inherently more complex behavior of merging vehicles compared to other vehicles, this research focuses on the merging decisions made by CAVs rather than other cooperative operations made by CAVs to thoroughly evaluate the potential effectiveness of CAVs. Therefore, we only consider scenarios where the merging vehicle is the only CAV within the merging vehicle group due to the fact that cooperative merging is highly dependent on the penetration

rates of CAVs and the comparatively limited role that reduced complexity plays in facilitating cooperation between the merging CAV and surrounding CAVs.

In this study, the continuous merging task is discretized into small decision steps, specifically 0.1 second, which is sufficient to control micro-level driving behaviors without resulting in computational wastage. We assume that the CAV can obtain motion information from its surrounding manually driven vehicles (MDVs). The complete merging process is defined as starting when the CAV enters the auxiliary lane from the on-ramp and ending when the CAV reaches the center line of the target lane (Lane 1).

To determine the specific composition of the merging vehicle group, we first analyze the potential changes in merging scenarios. Generally, changes related to the merging vehicle group can be divided into three cases:

Case 1: The spatial dynamics of the initial merging group change. However, the CAV can effectively manage them. These changes typically unfold as a successive process, during which the CAV continually collects data on all manually driven vehicles (MDVs) within the merging vehicle group. This continuous data collection enables the CAV to adapt accordingly.

Case 2: Certain surrounding vehicles separate from the initial merging vehicle group. This can be beneficial to the merge by enlarging the available space for the merge.

Case 3: Some new vehicles insert into the initial merging vehicle group, which may present great challenges. The insertion of the new vehicles may impose much stricter constraints and reduce the space available for merging, thus complicating the merging process.

To eliminate the possibility of Case 3, the merging vehicle group, as well as the range of CAV's data collection, should consist of the merging vehicle and more than six surrounding vehicles, i.e., the leading vehicle in Lane -1 (LA), the following vehicle in Lane -1 (FA), the leading vehicle in Lane 1 (LB), the vehicle leading LB in Lane 1 (LLB), the vehicle following in Lane 1 (FB), the vehicle following FB in Lane 1 (FFB), and any vehicles (if exist) in Lane 2 (C_x) that are longitudinally situated between LB and FB. During the merging process, vehicle LA, FA, LB, and FB will directly impact the merging decisions. Including vehicle LLB and FFB in the merging group assists in gap decision-making and mitigates the impact of Lane 1 overtaking on the merge. By incorporating vehicle C_x into the merging group and monitoring the lateral distance between vehicle C_x and the merging vehicle, the risk posed by Lane 2 vehicles changing lanes and merging into the gap designated for the merging vehicle is effectively reduced. Then, the complexity arising from the unpredictable changes in practical merging scenarios can be significantly reduced, since the space relationship between the merging CAV and MDVs in merging vehicle group is known in each decision step.

As shown in Fig. 2, a merging strategy framework is proposed, which divides the merging into longitudinal and lateral parts. Although many previous researches have shown

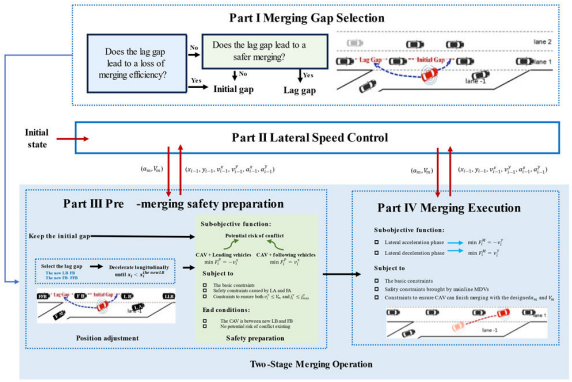

FIGURE 2. The proposed merging strategy framework.

that introducing vehicle direction can enable simultaneous lateral and longitudinal control of CAVs [25], [26], [27], this approach leads to model nonlinearity, which can compromise the efficiency of solving the model. Note that the longitudinal direction refers to the direction along the freeway, while the lateral direction refers to the direction vertical to the freeway. The longitudinal part ensures the merging safety, while the lateral part could improve the merging efficiency. Firstly, a merging gap selection method (Part I) is proposed, which helps CAV identify a safe merging gap without sacrificing efficiency. Subsequently, we introduce a conceptualized ideal ''lateral speed control'' strategy (Part II), designed to offer lateral guidance and enhance merging efficiency. Through this process, optimal lateral speed control parameters can be obtained and updated as the merging process progresses. Then, a two-stage merging procedure is proposed according to the above control parameters: the ''pre-merging safety preparation'' method (Part III) and the ''merging execution'' process (Part IV). In Part III, the CAV is controlled to adjust its speed longitudinally to eliminate potential conflicts. In Part IV, the CAV completes the whole merging process under the constraints of safety and comfort.

The goal of the merging strategy is to maximize the merging efficiency by minimizing merging time. The longitudinal and lateral speeds (v_i^x, v_i^y) at each decision step of the merging CAV are decision variables and the minimum merging time for each part is equal to the maximum speed under constraints. The main notations used in the model are summarized in Table 1.

A. PART I - MERGING GAP SELECTION

In this section, a method of merging gap selection is proposed for the merging CAV. As shown in Fig. 3, the merging gap between vehicle LB and FB when the merging CAV at the initial merging point is defined as the initial gap. However, due to the difference in vehicle speeds, the initial gap may be not the optimal one, so a gap selection method is developed for CAVs to select an optimal gap from a safety perspective.

Since the on-ramp vehicles generally move at a slightly slower speed than those on the mainline, it poses a risk for the merging CAV to attempt to overtake the leading vehicle

TABLE 1. List of notations.

Vehicle	Notation	Description	Unit
-	Δt	Decision time interval.	0.1s
	i	The i-th decision step.	-
Surrounding MDVs	H	The collection of surrounding MDVs in merging vehicle group, $H \in \{LA, FA, LB, FB, LLB, FFB, C_x\}$	-
	x_i^H	Longitudinal coordinate of H at the i-th decision step.	m
	y_i^H	Lateral coordinate of H at the i-th decision step.	m
	$v_i^{H,x}$	Longitudinal speed of H at the i-th decision step.	m/s
	w^H	The width of H.	m
Merging CAV	x_i	Longitudinal coordinate of CAV at the i-th decision step.	m
	y_i	Lateral coordinate of CAV at the i-th decision step.	m
	v_i^x	Longitudinal speed of CAV at the i-th decision step.	m/s
	v_i^y	Lateral speed of CAV at the i-th decision step.	m/s
	a_i^x	Longitudinal acceleration of CAV at the i-th decision step.	m/s^2
	a_i^y	Lateral acceleration of CAV at the i-th decision step.	m/s^2
	j_i^x	Longitudinal jerk of CAV at the i-th decision step.	m/s^3
	j_i^y	Lateral jerk of CAV at the i-th decision step.	m/s^3
	TTC_i^H	TTC between CAV and H at the i-th decision step.	s
	w^{CAV}	The width of CAV.	m

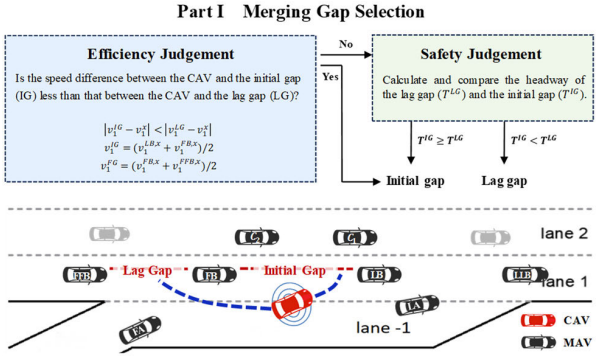

FIGURE 3. Workflow of the merging gap selection method.

to reach the adjacent lead gap. Then, the initial gap and the adjacent lag gap are suitable options for merging CAV to avoid spending too much time on speed adjustment [28]. As Fig. 3 shows, two judgment sessions are designed in Part I to assist the CAV in making its decision. In the efficiency judgement session, a new metric is proposed for the CAV to choose the suitable gap. It is well-understood that to achieve harmonious merging, CAVs should match the speed of the main traffic flow as closely as possible upon merging. Therefore, we calculate and compare the speed difference between the average speed of the vehicles that form the two gaps and the speed of the CAV at the beginning point of the merging process, as written in (1)-(4). A smaller speed difference indicates less need for speed adjustment for CAV, resulting in less time cost. If the speed difference between the initial gap and the CAV is smaller, the CAV is supposed to maintain the initial gap. Instead, it will continue assessing the safety of both the initial and lag gap based on the gap length.

$$v_1^{IG} = (v_1^{LB,x} + v_1^{FB,x}) \Big/ 2 \tag{1}$$

$$v_1^{LG} = (v_1^{FB,x} + v_1^{FFB,x}) \Big/ 2 \tag{2}$$

$$\Delta v^{IG} = \left| v_1^{IG} - v_1^x \right| \tag{3}$$

$$\Delta v^{LG} = \left| v_1^{LG} - v_1^x \right| \tag{4}$$

where $v_1^{LB,x}$, $v_1^{FB,x}$, $v_1^{FFB,x}$, and v_1^x are the longitudinal speed of vehicle LB, FB, FFB, and the CAV at the beginning point of the merging process, respectively. Although there might be a potential safety issue between MDVs with the following vehicle moving faster than the leading vehicle, this risk is eliminated because we consider the impact of the following vehicle's speed when assessing the safety of merging gaps. Additionally, the entire merging process is subject to safety constraints.

Studies related to merging gap safety assessment often rely on gap acceptance theory [29], where headway is commonly used as a metric to quantify the length safety of the gap, see (5). The longer the gap, the safer the merging process will be.

$$T_1^G = (x_1^l - x_1^f) \Big/ v_1^{f,x}, G \in \{IG, LG\} \tag{5}$$

where T_1^G is the headway of a gap (G) at the beginning point of the merging process, IG refers to the initial gap, LG refers to the lag gap, x_1^l is the X-coordinate of the leading vehicle that forms the gap at the beginning point, x_1^f is the X-coordinate of the following vehicle that forms the gap at the beginning point, and $v_1^{f,x}$ is the longitudinal speed of the following vehicle. If $T_1^{IG} \geq T_1^{LG}$, the CAV is expected to keep the initial gap (IG); if $T_1^{IG} < T_1^{LG}$, then lag gap (LG) is much safer and more suitable for CAV.

Obviously, the potential change in the vehicles consist of the two gaps are not reflected in the merging gap selection method. However, even in a realistic merging scenario, predicting the probability of lane-changing behavior of surrounding vehicles poses a formidable challenge, especially when the merging vehicle lacks adequate time to gather sufficient motion information. Meanwhile, the time invested in data collection can lead to excessive delays or, even worse, miss the optimal merging gap. Therefore, it is reasonable for the merging CAV to select the merging gap based solely on the initial state.

B. PART II - LATERAL SPEED CONTROL

To achieve a smooth and stable merging process, the merging CAV needs to plan its motion in advance at the beginning moment of merging. Noted that in Part II, we only discuss the lateral motion of the CAV, as this directly determines the execution of the merging process. As shown in Fig. 4, a lateral speed control method is designed for the merging CAV in this part, which offers ongoing guidance on lateral speed to facilitate the merging process. The method aims to generate the maximum lateral speed (V_m) and the maximum lateral acceleration or deceleration (a_m) for the merging CAV in the next merging operation.

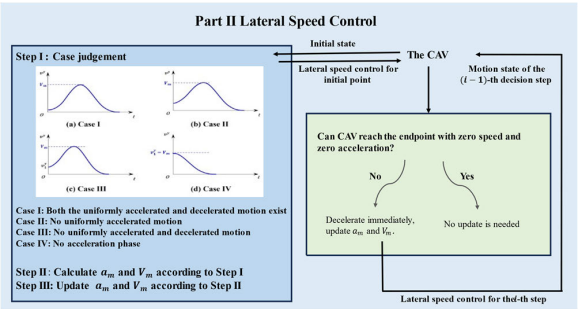

FIGURE 4. Workflow of lateral speed control.

At the beginning of the merge, the lateral speed of the CAV is v_1^y ($v_1^y \geq 0$), the lateral acceleration $a_1^y = 0$, and the CAV's lateral coordinate is y_1. Based on the previously defined concept of the merging process, the lateral target displacement of the CAV to complete the merge process is S^*, which can be calculated through (6).

$$S^* = y_T - y_1 \tag{6}$$

where y_T is the Y-coordinate of the center line of the target lane (Lane 1), y_1 is the Y-coordinate of the CAV at the beginning point.

Undoubtedly, smooth and uniform speed changes are best in the merging task to ensure maximum comfort and safety. Specifically, both the lateral speed and acceleration of the CAV should be reduced to 0 when it reaches the merging endpoint (the center line of the target lane). Then, an estimated ideal lateral $v-t$ curve can be represented as illustrated in Fig. 5, where the shaded area under the curve is consistently equal to S^*. The parameter a_m defines the curve's maximum slope, and V_m defines its peak.

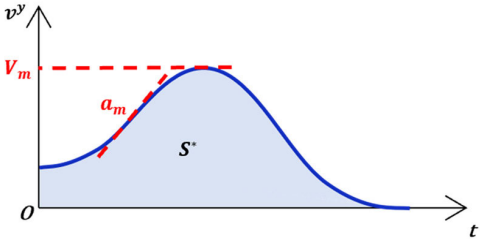

FIGURE 5. The $v^y - t$ curve of the CAV merging under an ideal environment.

Before solving the parameters a_m and V_m, the merging process is firstly simplified by setting $a_m = a_{\max}^y = 1\ \text{m/s}^2$ [30] temporarily, reported to Appendix A, assuming an idealized environment where there are no neighboring MDVs. Here, $a_{\max}^y$ is the maximum threshold of lateral acceleration or deceleration to ensure merging comfort.

As shown in Fig. 6, the motion in different cases can be characterized as a combination of various types of movement:

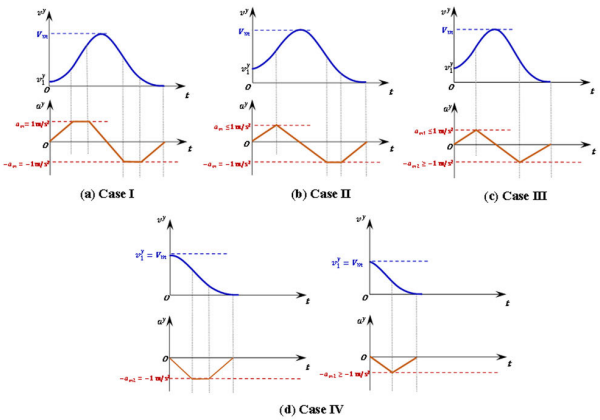

FIGURE 6. The motion curve of the CAV merging in different cases.

Case I: Accelerated motion with increasing acceleration - Uniformly accelerated motion - Accelerated motion with decreasing acceleration - Decelerated motion with increasing deceleration - Uniformly decelerated motion - Decelerated motion with decreasing deceleration.

Case II: Accelerated motion with increasing acceleration - Accelerated motion with decreasing acceleration - Decelerated motion with increasing deceleration - Uniform deceleration - Decelerated motion with decreasing deceleration.

Case III: Accelerated motion with increasing acceleration - Accelerated motion with decreasing acceleration - Decelerated motion with increasing deceleration - Decelerated motion with decreasing deceleration.

Case IV: Decelerated motion with increasing deceleration - Uniform deceleration (may exist) - Decelerated motion with decreasing deceleration.

The lateral displacement of the CAV in different cases can be obtained by calculating the area enclosed by the speed curve and the coordinate axis through (7)-(10), which corresponds to Case I-IV, respectively.

$$S_I = \frac{V_m^2}{a_m} + \frac{a_m V_m}{2j_{\max}^y} + \frac{a_m v_1^y}{2j_{\max}^y} - \frac{v_1^{y\,2}}{2a_m} \tag{7}$$

$$S_{II} = \frac{V_m + v_1^y}{\sqrt{j_{\max}^y}}\sqrt{V_m - v_1^y} + \frac{V_m^2}{2a_m} + \frac{a_m V_m}{2j_{\max}^y} \tag{8}$$

$$S_{III} = \frac{V_m + v_1^y}{\sqrt{j_{\max}^y}}\sqrt{V_m - v_1^y} + \frac{V_m}{\sqrt{j_{\max}^y}}\sqrt{V_m} \tag{9}$$

$$S_{IV} = \begin{cases} \dfrac{V_m^2}{2a_m} + \dfrac{a_m V_m}{2j_{\max}^y}, & \text{uniform deceration exists} \\ \dfrac{a_m V_m}{j_{\max}^y}, & \text{no uniform deceration} \end{cases} \tag{10}$$

where $j_{\max}^y$ is the maximum lateral jerk.

By setting $S = S^*$, and incorporating the constraints in (11)-(20), the crucial parameters a_m and V_m for different cases can be solved. Details of the judgment and solution process are provided in Appendix B.

$$v_{\min}^x \le v_i^x \le v_{\max}^x \tag{11}$$
$$0 \le v_i^y \le V_m \tag{12}$$
$$d_{\max}^x \le a_i^x \le a_{\max}^x \tag{13}$$
$$\left|a_i^y\right| \le a_m \tag{14}$$
$$j_i^x \le j_{\max}^x \tag{15}$$
$$j_i^y \le j_{\max}^y \tag{16}$$
$$v_i^x = v_{i-1}^x + a_{i-1}^x \Delta t \tag{17}$$
$$v_i^y = v_{i-1}^y + a_{i-1}^y \Delta t \tag{18}$$
$$x_i = x_{i-1} + v_{i-1}^x \Delta t + a_{i-1}^x \Delta t^2 \Big/ 2 \tag{19}$$
$$y_i = y_{i-1} + v_{i-1}^y \Delta t + a_{i-1}^y \Delta t^2 \Big/ 2 \tag{20}$$

In (11), $v_{\min}^x = 16.7$ m/s and $v_{\max}^x = 27.7$ m/s are the upper and lower bounds of the lateral speed constraint, according to the real-world speed limits on freeways. Equation (12) is the lateral speed constraint according to the calculation of V_m. Equations (13)-(14) are the longitudinal and lateral acceleration constraints to ensure passengers' comfort, where $d_{\max}^x = -2\text{m/s}^2$ and $a_{\max}^x = 1.25\ \text{m/s}^2$ are the maximum longitudinal deceleration and acceleration [31], a_m is the maximum lateral acceleration. In (15)-(16), $j_{\max}^x = 9.75\ \text{m/s}^3$ and $j_{\max}^y = 5.10\ \text{m/s}^3$ are the maximum longitudinal and lateral jerk, respectively [32]. Equations (17)-(20) are physical kinematics constraints.

Though a_m and V_m can be obtained at the beginning point of the merging process through the above steps, the disturbance caused by the other MDVs in the practical merging process must be taken into account. Therefore, the two parameters must be checked and updated in each decision step according to the actual conditions to ensure that the CAV has zero lateral speed and lateral acceleration at the endpoint, which is crucial for stable merging. As for the $(i-1)$-th step, the remaining displacement is

$$S_R^* = y_T - y_{i-1} \tag{21}$$

where y_T is the Y-coordinate of the center line of the target lane (Lane 1).

Assuming that the CAV begins to decelerate from its current lateral speed and acceleration until both reach zero, the displacement during this deceleration will be (22), as shown at the bottom of the next page, where $v_{i-1}^y + {a_{i-1}^y}^2 \Big/ 2j_{\max}^y > a_m^2 / j_{\max}^y$ refers to the case where uniform decelerated motion exists in above deceleration, and $v_{i-1}^y + {a_{i-1}^y}^2 \Big/ 2j_{\max}^y \le a_m^2 / j_{\max}^y$ refers to the case without uniform decelerated motion.

Once $S' \ge S_R^*$, the CAV has to decelerate immediately and the value of a_m and V_m need to be updated as follows:

$$V_m' = v_{i-1}^y + {a_{i-1}^y}^2 \Big/ 2j_{\max}^y \tag{23}$$
$$V_m' = v_{i-1}^y + {a_{i-1}^y}^2 \Big/ 2j_{\max}^y \tag{24}$$
$$a_{m2} = \begin{cases} a_m, & V_m' > a_m^2 \Big/ j_{\max}^y \\ \sqrt{V_m' j_{\max}^y}, & V_m' \le a_m^2 \Big/ j_{\max}^y \end{cases} \tag{25}$$

where V_m' is the updated value of V_m, a_{m1} is the updated value of a_m for the acceleration phase, and a_{m2} is the updated value of a_m for the deceleration phase.

This method ensures that the CAV can adapt its merging parameters in response to any unforeseen circumstances or the presence of surrounding MDVs, optimizing the safety and efficiency of the merging process. In summary, lateral speed control provides the CAV with continuous guidance on the lateral speed at each decision step to ensure an effective merging process.

C. PART III - PRE-MERGING SAFETY PREPARATION

Part III focuses on establishing the essential safety constraints for a successful merge. In this phase, the merging CAV adjusts its longitudinal speed to ensure safe entry into the selected gap before the merging process begins. The reciprocal of the Time-To-Collision (TTC) metric is employed as the safety constraint. Two vehicles are considered safe if the TTC between them is less than 0 s or greater than 4 s [33], so the safety minimum threshold value of $(TTC)^{-1}$ is 0.25.

As shown in Fig. 7, whether the CAV chooses the initial gap or lag gap, it needs to reach a safe state and obey the safety constraints before the merging process begins (the green part). If any potential conflict risk exists between the CAV and its surrounding MDVs (LA, LB, FA, FB, and C_x if existing), the CAV needs to adjust its longitudinal speed to keep absolute safe. The difference is that if the CAV chooses the lag gap as the merging gap, it is required to adjust its speed longitudinally to reach the lag gap (the blue part) before the green part, and the new FB is the initial FFB, and the new LB is the initial FB. During the pre-merging safety preparation, driven by the goal of an efficient merging, the sub-objective function of this part for each decision step (F_i^P) can be expressed as

$$\min F_i^P = \begin{cases} -v_i^x, & dir^x = 1 \\ v_i^x, & dir^x = 2 \end{cases} \tag{26}$$

where $dir^x = 1$ means the CAV needs to accelerate and $dir^x = 2$ means the CAV needs to decelerate. The value of dir^x is determined by both the merging gap selection and the position of MDVs in the mainline that may bring a potential conflict to the CAV.

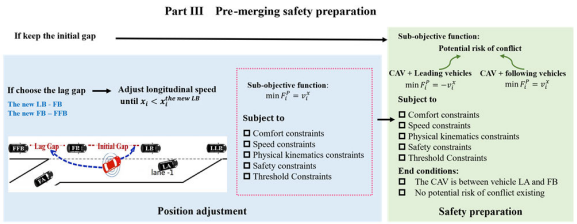

FIGURE 7. The process of pre-merging safety preparation.

In addition to the basic constraints (11)-(20), other constraints are shown below.

$$(TTC_i^{LA})^{-1} = \frac{v_i^x - v_i^{LA,x}}{x_i^{LA} - x_i} \leq 0.25 \tag{27}$$

$$(TTC_i^{FA})^{-1} = \frac{v_i^{FA,x} - v_i^x}{x_i - x_i^{FA}} \leq 0.25 \tag{28}$$

$$v_{\max}^x - v_i^x \geq a_i^{x2} \Big/ 2j_{\max}^x, dir^x = 1 \tag{29}$$

$$v_i^x - v_{\min}^x \geq a_i^{x2} \Big/ 2j_{\max}^x, dir^x = 2 \tag{30}$$

Equations (27)-(28) are the safety constraints related to vehicle LA and FA. Equations (29)-(30) are set to prevent the CAV from exceeding the range of speed constraints due to the constraint on longitudinal jerk during longitudinal acceleration and deceleration. Generally, the lateral distance for vehicles on the freeway is suggested to be more than 1.5 m to avoid the risk of side collision. We consider only the physical dimensions of vehicles in the lateral direction, as the longitudinal distance between vehicles is significantly greater than vehicle length. Specifically, once $y_i - y_i^H > 1.5 + (w^{CAV} + w^H)/2, H \in \{LA, FA\}$ satisfied, constraints (27)-(28) can be abandoned. In addition, all these constraints can be rearranged into linear constraints. Once the following conditions (see (31)-(33)) are met, the longitudinal preparation is over. And the CAV is capable of executing merging maneuvers.

$$x_i^{FB} < x_i < x_i^{LB} \tag{31}$$

$$(TTC_i^B)^{-1} = \begin{cases} \dfrac{v_i^{FB,x} - v_i^x}{x_i - x_i^{FB}} \leq 0.25, & dir^x = 1 \\ \dfrac{v_i^x - v_i^{LB,x}}{x_i^{LB} - x_i} \leq 0.25, & dir^x = 2 \end{cases} \tag{32}$$

$$(TTC_i^C)^{-1} = \begin{cases} \dfrac{v_i^{FC,x} - v_i^x}{x_i - x_i^{FC}} \leq 0.25, & dir^x = 1 \\ \dfrac{v_i^x - v_i^{LC,x}}{x_i^{LC} - x_i} \leq 0.25, & dir^x = 2 \end{cases} \tag{33}$$

where LC is the leading C_x if existing and FC is the following C_x if existing. Eq. (31) guarantees that the CAV merges into the selected gap. When Eq. (32)-(33) are satisfied, it states that the potential risk of conflict has been eliminated.

D. PART IV - MERGING EXECUTION

Part IV controls the CAV to complete the merging process. According to the previous analysis of the merging under ideal conditions, we can consider the lateral merging process as a two-phase movement: accelerating to V_m and decelerating from V_m to 0. To minimize the merging time, the sub-objective of this part (F_i^M) at each decision step is

$$\min F_i^M = \begin{cases} -v_i^y, & dir^y = 1 \\ v_i^y, & dir^y = 2 \end{cases} \tag{34}$$

where dir^y is the direction of the CAV's lateral acceleration, $dir^y = 1$ means the CAV needs to accelerate laterally to V_m, and $dir^y = 2$ means the CAV needs to decelerate laterally to 0. The constraints for this part include (12)-(21) and (27)-(28), and the rest are shown as follows:

$$(TTC_i^{LB})^{-1} = \frac{v_i^x - v_i^{LB,x}}{x_i^{LB} - x_i} \leq 0.25 \tag{35}$$

$$(TTC_i^{FB})^{-1} = \frac{v_i^{FB,x} - v_i^x}{x_i - x_i^{FB}} \leq 0.25 \tag{36}$$

$$(TTC_i^{C_x})^{-1} = \frac{v_i^x - v_i^{C_x,x}}{x_i^{C_x} - x_i} \leq 0.25 \tag{37}$$

$$V_m - v_i^y \geq a_i^{y2} \Big/ 2j_{\max}^y, dir^y = 1 \tag{38}$$

$$V_m - v_i^y \geq a_i^{y2} \Big/ 2j_{\max}^y, dir^y = 1 \tag{39}$$

Equations (35)-(37) are the safety constraints brought by MDVs in the mainline. Equations (38)-(39) are set to ensure the CAV can merge with the designed a_m and V_m. Note that, equation (37) can be abandoned once $y_i - y_i^H > 1.5 + (w^{CAV} + w^{C_x})/2$ is satisfied, which is the same as (27)-(28). In this part, driven by (34), the CAV can achieve a safe, comfortable, and efficient merging process.

III. NUMERICAL EXPERIMENT

The empirical trajectory dataset used in this study was collected at a 1,200 m long freeway segment of Delft on the

$$S' = \begin{cases} \dfrac{1}{2}(2v_{i-1}^y + \dfrac{a_{i-1}^{y\,2}}{2j_{\max}^y})\dfrac{a_{i-1}^y}{j_{\max}^y} + \dfrac{1}{2}(v_{i-1}^y + \dfrac{a_{i-1}^{y\,2}}{2j_{\max}^y})(\dfrac{v_{i-1}^y}{a_m} + \dfrac{a_{i-1}^{y\,2}}{2a_m j_{\max}^y} + \dfrac{a_m}{j_{\max}^y}), v_{i-1}^y + \dfrac{a_{i-1}^{y\,2}}{2j_{\max}^y} > \dfrac{a_m^2}{j_{\max}^y} \\ \dfrac{1}{2}(2v_{i-1}^y + \dfrac{a_{i-1}^{y\,2}}{2j_{\max}^y})\dfrac{a_{i-1}^y}{j_{\max}^y} + \dfrac{1}{2}(v_{i-1}^y + \dfrac{a_{i-1}^{y\,2}}{2j_{\max}^y})\sqrt{(v_{i-1}^y + \dfrac{a_{i-1}^{y\,2}}{2j_{\max}^y})j_{\max}^y}, v_{i-1}^y + \dfrac{a_{i-1}^{y\,2}}{2j_{\max}^y} \leq \dfrac{a_m^2}{j_{\max}^y} \end{cases} \tag{22}$$

6th of June and the 7th of July 2016 [34]. The raw vehicle video was taken during the evening peak hour for 30 minutes and processed every 0.1 seconds. The trajectory data includes vehicle position, speed, direction, and physical characteristics such as width and length. As shown in Fig. 8 (a), the freeway segment has three main lanes, one acceleration lane, and one on-ramp. The research focus of this study is merging behaviors, along with other vehicle behaviors that may influence it. Therefore, the analysis is confined to the shaded area in the Fig. 8(b), which includes Lane -1, Lane 1, and Lane 2.

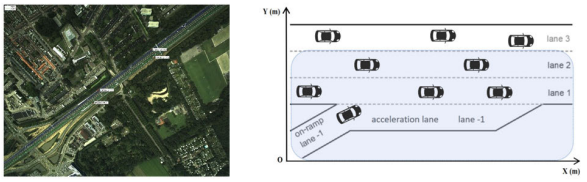

(a) Aerial photo of the segment (b) Schematic of the segment

FIGURE 8. Illustration of the freeway segment.

Owing to the observed noise within the dataset, the following data pre-processing measures are adopted. Firstly, we eliminate abnormal vehicle trajectories, such as trajectories that have inconsistencies with the relative positions of vehicles and their actual positions. The moving average method is applied to smooth the coordinate data of vehicles, and the speed and acceleration are recalculated according to the smoothed coordinates. A total of 255 multi-lane merging scenarios is extracted based on the following extraction rules:

(1) The merging vehicle groups are identified and extracted according to the previous definition in Section II. Note that all the leading and following vehicles are the nearest ones to the merging vehicle.

(2) Given that the merging process is dynamic, the relative vehicle relationships also change continuously. Consequently, we extract trajectory data considering the proximal vehicles to the merging one at every time step, mirroring the perception capabilities of a CAV. Detailed operations are shown in Fig. 9.

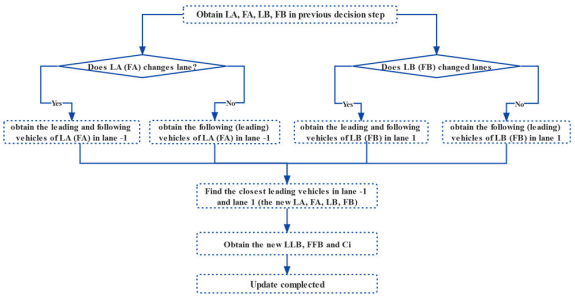

FIGURE 9. The update operation for the merging vehicle group at each decision step.

IV. RESULTS AND DISCUSSIONS

The proposed model is employed in empirical merging scenarios following the steps below. Step A: Identification and extraction of merging scenarios from the trajectory dataset. Step B: Replacement of the merging MDV in each scenario with CAV and assigning the initial state of the MDV to CAV. CAVs can gather information about surrounding vehicles through roadside units [35], [36]. Step C: The merging strategies are formulated for CAVs using the proposed model. The model is solved by the linprog function in MATLAB, which is a toolkit used for solving linear optimization.

A. MERGING TIME AND TRAJECTORIES

Among the 255 merging scenarios, 254 CAVs' optimal merging trajectories are obtained, and one CAV fails to find a solution. The main reason for the failure lies in the extracted scenario, where the initial TTC between the CAV and its surrounding vehicle is close to the safety threshold. Due to the strict comfort constraints, the CAV cannot avoid triggering the threshold in such cases. However, it should be noted that in real-world scenarios, vehicle movements occur as continuous processes, and sudden appearances are unlikely to occur. Even in such urgent situations, there is no need to consider the conflict between strict comfort constraints (see (13)-(16)) and other constraints.

In Fig. 10 (a), the merging time of CAVs and MDVs are compared, showing that most CAVs can merge more efficiently than MDVs. It can be found that most CAVs can complete the merging task within 5 s, while most of the MDVs' merging time falls in the range of 5-10 s. The number and value of outliers for CAVs are significantly lower than those of MDVs, which proves the stability of the proposed model. Only a few of the CAVs merge a little more slowly than their corresponding merging MDVs, mainly caused by the strict comfort constraints.

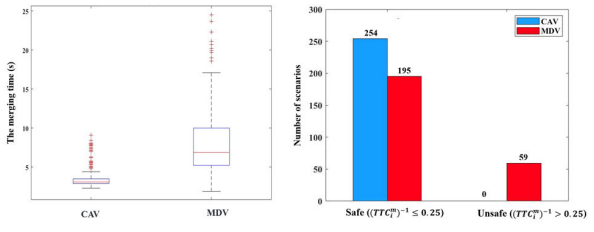

(a) Merging time (b) The most dangerous *TTC*

FIGURE 10. Comparison of merging efficiency and safety between CAVs and MDVs.

As illustrated in Fig. 10 (b), the most dangerous *TTC* (TTC_i^m) between the merging vehicles and their surrounding vehicles during the merging process are calculated and compared. Vehicles are categorized into "safe" and "unsafe" based on whether this TTC_i^m falls within the 0-4 second range. The data demonstrate that CAVs are effective in enhancing the safety of the merging process, as none of the CAVs experience a dangerous moment throughout the merging process.

Fig. 11 compares the trajectories of the CAVs with the merging MDVs. The color of trajectories is determined by

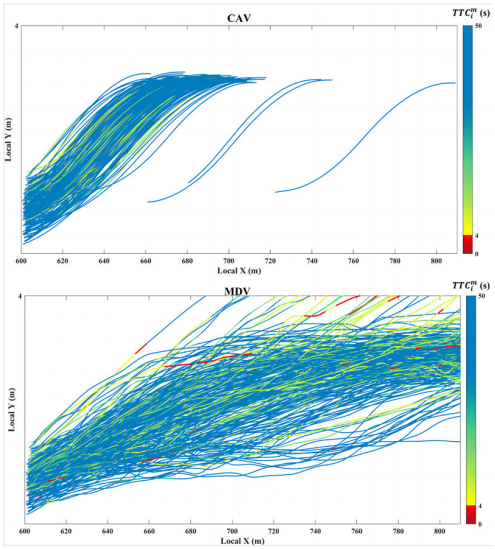

FIGURE 11. The merging trajectories of MDVs and CAVs.

the safety of the merging process. If there is a risk of conflict between the CAV and a specific MDV in the merging vehicle group, indicated by $0 < TTC < 4$, that segment of the trajectory is displayed in red. The trajectory color transitions from yellow to blue, representing increasing levels of safety. And shows that the CAVs' trajectories are much smoother and safer. The Y-coordinates of the CAVs at the merging endpoints are stable between 1.9 and 2.4 m (the target position is $y_T = 1.8$ m), while some MDVs continue to perform lateral movements even after the merging process has been completed.

B. MERGING GAP SELECTION

Among the 254 CAVs, 45 chose the lag gap rather than the initial gap (see Fig. 12), among which 7 corresponding MDVs also made the same choice.

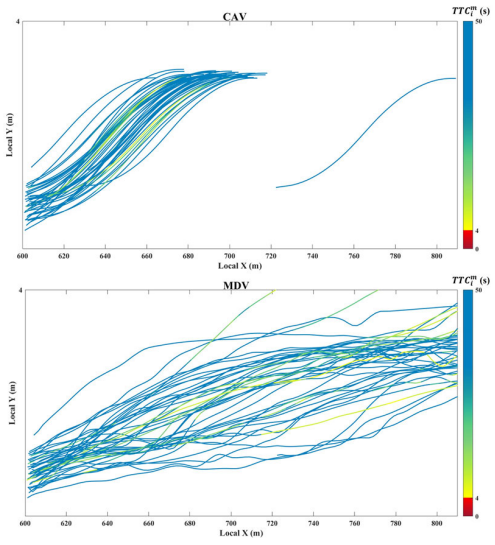

FIGURE 12. Comparison of CAVs who select lag gap and their corresponding MDVs.

The results show that CAVs with the lag gap selection can complete the merging faster and smoother. Note that, the selection by the model is optimal for the initial point moment. However, it may not be the optimal solution for the whole merging process as subsequent merging scenario changes. Nevertheless, even in such cases, CAVs can improve merging efficiency and smoothness through gap selection based on the initial point.

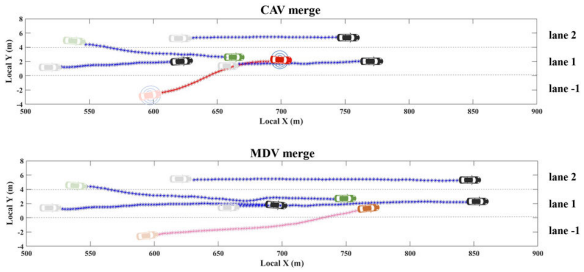

FIGURE 13. Comparison of the CAV who selects the lag gap and its corresponding MDV.

C. CASE ANALYSIS

Fig. 13 shows the merging process of a CAV (highlighted in red in the upper subplot) and its corresponding MDV (highlighted in orange in the lower subplot) under the same merging scenario. The vehicle on Lane 2 (green vehicle) changed to Lane 1 simultaneously with the merging vehicle beginning the merging process and inserted into the target gap of the CAV. Due to the close distance of the green vehicle to the rear vehicle in Lane 1, a rapid lane change to a spot ahead of the green vehicle's estimated arrival location is a better choice. The figure reveals that the MDV (orange car) conducted a more cautious merging process than the CAV, which makes it highly exposed to a rear-end collision risk at the endpoint. However, due to the CAV's earlier merging time and position, it keeps a safe distance from the green vehicle, making the merge both safer and more efficient.

V. CONCLUSION

In this study, a merging strategy framework taking into account the multi-lane scenario is proposed for merging CAVs in mixed traffic flow scenarios, which takes merging efficiency as the objective and merging safety and comfort as constraints. The framework consists of four key parts. First, a "Merging Gap Selection Method" (Part I) assists CAV in identifying a more suitable gap for merging. Second, an ideal "Lateral Speed Control" strategy (Part II) is designed to offer lateral guidance and enhance merging efficiency by giving optimal lateral speed control parameters. Third, a "Pre-Merging Safety Preparation" method (Part III) controls the CAV to adjust its speed longitudinally to eliminate potential conflicts. Lastly, the "Merging Execution" phase (Part IV) ensures that the CAV completes the whole merging process under the constraints of safety and comfort. To verify the effectiveness of the model, we extract 255 merging scenarios from the empirical trajectory data of Delft and

replace the merging MDV in each scenario with CAV. The results indicate that under the multi-lane scenarios, the proposed method shows better performance in formulating more effective merging trajectories than MDVs.

In future work, taking the communication delay into account is essential for enhancing operational stability. Acknowledging and mitigating the impact of these delays in CAV decision-making is vital for maintaining merge efficiency and reducing the likelihood of system disruptions. Additionally, the effectiveness of CAV merging strategies must be validated across different on-ramp structures, including variations in length, gradient, and entry angles, to ensure comprehensive applicability to infrastructure diversity.

APPENDIX A

PROOF: THE LARGER THE IS, THE SHORTER THE MERGING TAKES

The verification is carried out by reductio. Firstly, the inverse proposition is set as the larger the a_m is, the longer merging takes. The time both consumed in the acceleration (t_1) and deceleration phases (t_2) is calculated as follows in respective:

$$t_1 = \frac{V_m - v_1^y - a_m^2/j_{\max}^y}{a_m} + \frac{2a_m}{j_{\max}^y} = \frac{V_m - v_1^y}{a_m} + \frac{a_m}{j_{\max}^y} \tag{A.1}$$

$$t_2 = \frac{V_m - a_m^2/j_{\max}^y}{a_m} + \frac{2a_m}{j_{\max}^y} = \frac{V_m}{a_m} + \frac{a_m}{j_{\max}^y} = t_1 + \frac{v_1^y}{a_m} \tag{A.2}$$

$$t_1 + t_2 = 2t_1 + v_1^y/a_m \tag{A.3}$$

Thus, the time taken by the merging process is shown in (A.3). According to the inverse proposition, it is known that $t_1 + t_2$ increases with a_m. When a_m increases, the left-hand side of (A.3) ($t_1 + t_2$) goes higher, and the term v_1^y/a_m on the right-hand side of (A.3) goes down. To make (A.3) true, t_1 has to increase along with a_m. The lateral displacement of the CAV can be denoted by

$$\begin{aligned} S^* &= y_T - y_1 = (V_m + v_1^y)t_1/2 + V_m t_2/2 \\ &= v_1^y t_1/2 + V_m(t_1 + t_2)/2 \end{aligned} \tag{A.4}$$

Based on the above inference (t_1 has to increase along with a_m), when a_m increases, the term $v_1^y t_1/2$ on the right-hand side of (A.4) increases. To make (A.4) true, the term $V_m(t_1 + t_2)/2$ on the right-hand side of (A.4) must decrease since the left-hand side is fixed. Hence, it follows that V_m would decrease as a_m increases. However, V_m can be calculated as

$$V_m = v_1^y + a_m^2/2j_{\max}^y + a_m t_1 \tag{A.5}$$

Obviously, V_m increases along with a_m, which contradicts the previous inference (V_m decreases as a_m increases). Hence, the inverse proposition (the larger the a_m is, the longer merging takes) is not true, and the original proposition is proved.

APPENDIX B

See table 2.

TABLE 2. The specific operations for updating a_m and V_m.

Case	Judgment condition	The updated value of a_m and V_m [a]
Case I	$V_m > v_1^y + \frac{a_m^2}{2j_{\max}^y}$	$a_{m1} = a_m$ $a_{m2} = a_m$ $V_m' = V_m$
Case II	$\frac{a_m^2}{j_{\max}^y} < V_m \le v_1^y + \frac{a_m^2}{2j_{\max}^y}$	$a_{m1} = \sqrt{(V_m' - v_1^y)j_{\max}^y}$ $a_{m2} = a_m$ Calculate V_m' by solving $S_T = \frac{V_m + v_1^y}{j_{\max}^y}\sqrt{V_m - v_1^y} + \frac{V_m^2}{2a_m} + \frac{a_m V_m}{2j_{\max}^y}$
Case III	$v_1^y < V_m \le \frac{a_m^2}{j_{\max}^y}$	$a_{m1} = \sqrt{(V_m' - v_1^y)j_{\max}^y}$ $a_{m2} = \sqrt{V_m' j_{\max}^y}$ Calculate V_m' by solving $S_T = \frac{V_m + v_1^y}{\sqrt{j_{\max}^y}}\sqrt{V_m - v_1^y} + \frac{V_m}{\sqrt{j_{\max}^y}}\sqrt{V_m}$
Case IV	$V_m \le v_1^y$	When $v_1^y < a_m^2/j_{\max}^y$, $a_{m2} = S_T j_{\max}^y / V_m'$ When $v_1^y \ge a_m^2/j_{\max}^y$, calculate a_{m2} by solving $S_T = \frac{1}{2}(\frac{V_m'}{a_m} + \frac{a_m}{j_{\max}^y})V_m'$, where $V_m' = v_1^y$

[a] a_{m1} is the updated value of a_m for the acceleration phase, a_{m2} is the updated value of a_m for the deceleration phase, V_m' is the updated value of V_m.

REFERENCES

[1] J. Sun, J. Zhang, and H. M. Zhang, "Investigation of the early-onset breakdown phenomenon at urban expressway bottlenecks in Shanghai," *Transportmetrica B, Transp. Dyn.*, vol. 2, no. 3, pp. 215–228, Sep. 2014, doi: 10.1080/21680566.2014.932262.

[2] N. Chen, B. van Arem, T. Alkim, and M. Wang, "A hierarchical model-based optimization control approach for cooperative merging by connected automated vehicles," *IEEE Trans. Intell. Transp. Syst.*, vol. 22, no. 12, pp. 7712–7725, Dec. 2021, doi: 10.1109/TITS.2020.3007647.

[3] B. Sun, G. Ma, J. Song, Z. Cheng, and W. Wang, "Driving safety field modeling focused on heterogeneous traffic flows and cooperative control strategy in highway merging zone," *Phys. A, Stat. Mech. Appl.*, vol. 630, Nov. 2023, Art. no. 129215, doi: 10.1016/j.physa.2023.129215.

[4] E. Amini, A. Omidvar, and L. Elefteriadou, "Optimizing operations at freeway weaves with connected and automated vehicles," *Transp. Res. C, Emerg. Technol.*, vol. 126, May 2021, Art. no. 103072, doi: 10.1016/j.trc.2021.103072.

[5] A. Talebpour and H. S. Mahmassani, "Influence of connected and autonomous vehicles on traffic flow stability and throughput," *Transp. Res. C, Emerg. Technol.*, vol. 71, pp. 143–163, Oct. 2016, doi: 10.1016/j.trc.2016.07.007.

[6] J. Guanetti, Y. Kim, and F. Borrelli, "Control of connected and automated vehicles: State of the art and future challenges," *Annu. Rev. Control*, vol. 45, pp. 18–40, May 2018, doi: 10.1016/j.arcontrol.2018.04.011.

[7] Y. Liu, H. Wang, C. Dong, and Y. Chen, "A centralized relaxation strategy for cooperative lane change in a connected environment," *Phys. A, Stat. Mech. Appl.*, vol. 624, Aug. 2023, Art. no. 128934, doi: 10.1016/j.physa.2023.128934.

[8] H. Xu, S. Feng, Y. Zhang, and L. Li, "A grouping-based cooperative driving strategy for CAVs merging problems," *IEEE Trans. Veh. Technol.*, vol. 68, no. 6, pp. 6125–6136, Jun. 2019, doi: 10.1109/TVT.2019.2910987.

[9] J. Ding, L. Li, H. Peng, and Y. Zhang, "A rule-based cooperative merging strategy for connected and automated vehicles," *IEEE Trans. Intell. Transp. Syst.*, vol. 21, no. 8, pp. 3436–3446, Aug. 2020, doi: 10.1109/TITS.2019.2928969.

[10] L. C. Davis, "Optimal merging into a high-speed lane dedicated to connected autonomous vehicles," *Phys. A, Stat. Mech. Appl.*, vol. 555, Oct. 2020, Art. no. 124743, doi: 10.1016/j.physa.2020.124743.

[11] Y. Xue, X. Zhang, Z. Cui, B. Yu, and K. Gao, "A platoon-based cooperative optimal control for connected autonomous vehicles at highway on-ramps under heavy traffic," *Transp. Res. C, Emerg. Technol.*, vol. 150, May 2023, Art. no. 104083.

[12] W. Cao, M. Mukai, T. Kawabe, H. Nishira, and N. Fujiki, "Cooperative vehicle path generation during merging using model predictive control with real-time optimization," *Control Eng. Pract.*, vol. 34, pp. 98–105, Jan. 2015, doi: 10.1016/j.trc.2023.104083.

[13] J. Rios-Torres and A. A. Malikopoulos, "Automated and cooperative vehicle merging at highway on-ramps," *IEEE Trans. Intell. Transp. Syst.*, vol. 18, no. 4, pp. 780–789, Apr. 2017, doi: 10.1109/TITS.2016.2587582.

[14] I. A. Ntousakis, I. K. Nikolos, and M. Papageorgiou, "Optimal vehicle trajectory planning in the context of cooperative merging on highways," *Transp. Res. C, Emerg. Technol.*, vol. 71, pp. 464–488, Oct. 2016, doi: 10.1016/j.trc.2016.08.007.

[15] C. Letter and L. Elefteriadou, "Efficient control of fully automated connected vehicles at freeway merge segments," *Transp. Res. C, Emerg. Technol.*, vol. 80, pp. 190–205, Jul. 2017, doi: 10.1016/j.trc.2017.04.015.

[16] Z. Tang, H. Zhu, X. Zhang, M. Iryo-Asano, and H. Nakamura, "A novel hierarchical cooperative merging control model of connected and automated vehicles featuring flexible merging positions in system optimization," *Transp. Res. C, Emerg. Technol.*, vol. 138, May 2022, Art. no. 103650, doi: 10.1016/j.trc.2022.103650.

[17] S. Fukuyama, "Dynamic game-based approach for optimizing merging vehicle trajectories using time-expanded decision diagram," *Transp. Res. C, Emerg. Technol.*, vol. 120, Nov. 2020, Art. no. 102766, doi: 10.1016/j.trc.2020.102766.

[18] R. Pueboobpaphan, F. Liu, and B. van Arem, "The impacts of a communication based merging assistant on traffic flows of manual and equipped vehicles at an on-ramp using traffic flow simulation," in *Proc. 13th Int. IEEE Conf. Intell. Transp. Syst.*, Sep. 2010, pp. 1468–1473, doi: 10.1109/ITSC.2010.5625245.

[19] J. Rios-Torres and A. A. Malikopoulos, "Impact of partial penetrations of connected and automated vehicles on fuel consumption and traffic flow," *IEEE Trans. Intell. Vehicles*, vol. 3, no. 4, pp. 453–462, Dec. 2018, doi: 10.1109/TIV.2018.2873899.

[20] Y. Zhou, M. E. Cholette, A. Bhaskar, and E. Chung, "Optimal vehicle trajectory planning with control constraints and recursive implementation for automated on-ramp merging," *IEEE Trans. Intell. Transp. Syst.*, vol. 20, no. 9, pp. 3409–3420, Sep. 2019, doi: 10.1109/TITS.2018.2874234.

[21] Y. Zhou, E. Chung, A. Bhaskar, and M. E. Cholette, "A state-constrained optimal control based trajectory planning strategy for cooperative freeway mainline facilitating and on-ramp merging maneuvers under congested traffic," *Transp. Res. C, Emerg. Technol.*, vol. 109, pp. 321–342, Dec. 2019, doi: 10.1016/j.trc.2019.10.017.

[22] M. Karimi, C. Roncoli, C. Alecsandru, and M. Papageorgiou, "Cooperative merging control via trajectory optimization in mixed vehicular traffic," *Transp. Res. C, Emerg. Technol.*, vol. 116, Jul. 2020, Art. no. 102663, doi: 10.1016/j.trc.2020.102663.

[23] S. Karbalaieali, O. A. Osman, and S. Ishak, "A dynamic adaptive algorithm for merging into platoons in connected automated environments," *IEEE Trans. Intell. Transp. Syst.*, vol. 21, no. 10, pp. 4111–4122, Oct. 2020, doi: 10.1109/TITS.2019.2938728.

[24] J. Zhu, I. Tasic, and X. Qu, "Flow-level coordination of connected and autonomous vehicles in multilane freeway ramp merging areas," *Multimodal Transp.*, vol. 1, no. 1, Mar. 2022, Art. no. 100005, doi: 10.1016/j.multra.2022.100005.

[25] J. Zhao, V. L. Knoop, J. Sun, Z. Ma, and M. Wang, "Unprotected left-turn behavior model capturing path variations at intersections," *IEEE Trans. Intell. Transp. Syst.*, vol. 24, no. 9, pp. 9016–9030, Sep. 2023, doi: 10.1109/TITS.2023.3270962.

[26] J. Zhao, V. L. Knoop, and M. Wang, "Two-dimensional vehicular movement modelling at intersections based on optimal control," *Transp. Res. B, Methodol.*, vol. 138, pp. 1–22, Aug. 2020, doi: 10.1016/j.trb.2020.04.001.

[27] Y. Bichiou and H. A. Rakha, "Developing an optimal intersection control system for automated connected vehicles," *IEEE Trans. Intell. Transp. Syst.*, vol. 20, no. 5, pp. 1908–1916, May 2019, doi: 10.1109/TITS.2018.2850335.

[28] K. Ahmed, M. Ben-Akiva, H. Koutsopoulos, and R. Mishalani, "Models of freeway lane changing and gap acceptance behavior," *Transp. Traffic Theory*, vol. 13, pp. 501–515, Jan. 1996.

[29] Z. Zheng, "Recent developments and research needs in modeling lane changing," *Transp. Res. Part B: Methodol.*, vol. 60, pp. 16–32, Feb. 2014, doi: 10.1016/j.trb.2013.11.009.

[30] L. Svensson and J. Eriksson, "Tuning for ride quality in autonomous vehicle: Application to linear quadratic path planning algorithm," M.S. thesis, Dept. Elect. Comput. Eng., Uppsala Univ., Uppsala, Sweden, Jun. 2015.

[31] K. Fitzpatrick, L. Elefteriadou, and D. W. Harwood, "Speed prediction for two-lane rural highways," *FHWA-RD*, vol. 171, no. 99, pp. 1–217, 2000.

[32] Y. Guo, Y. Su, R. Fu, and W. Yuan, "Influence of lane-changing maneuvers on passenger comfort of intelligent vehicles," *China J. Highway Transport*, vol. 35, no. 5, pp. 221–230, 2022, doi: 10.19721/j.cnki.1001-7372.2022.05.021.

[33] S. M. S. Mahmud, L. Ferreira, M. S. Hoque, and A. Tavassoli, "Application of proximal surrogate indicators for safety evaluation: A review of recent developments and research needs," *IATSS Res.*, vol. 41, no. 4, pp. 153–163, Dec. 2017, doi: 10.1016/j.iatssr.2017.02.001.

[34] A. van Beinum, H. Farah, F. Wegman, and S. Hoogendoorn, "Driving behaviour at motorway ramps and weaving segments based on empirical trajectory data," *Transp. Res. C, Emerg. Technol.*, vol. 92, pp. 426–441, Jul. 2018, doi: 10.1016/j.trc.2018.05.018.

[35] Y. Li, Z. Chen, Y. Yin, and S. Peeta, "Deployment of roadside units to overcome connectivity gap in transportation networks with mixed traffic," *Transp. Res. C, Emerg. Technol.*, vol. 111, pp. 496–512, Feb. 2020, doi: 10.1016/j.trc.2020.01.001.

[36] Y. Li, Y. Ma, and Z. Chen, "How can connected and automated vehicles improve merging efficiency at freeway on-ramps?" *Transportmetrica A, Transp. Sci.*, vol. 20, no. 2, pp. 1–27, Nov. 2022, doi: 10.1080/23249935.2022.2149286.

YE LI received the B.Eng. and Ph.D. degrees in transportation planning and management from Southeast University, Nanjing, China, in 2014 and 2019, respectively. He is currently with the School of Traffic and Transportation Engineering, Central South University, Changsha, China, as an Associate Professor. He has published over 30 articles in international journals, such as *Journal of Safety Research*, *Accident Analysis and Prevention*, *Transportation Research—C: Emerging Technologies*, and IEEE TRANSACTIONS ON INTELLIGENT TRANSPORTATION SYSTEMS. His research interests include traffic safety and intelligent transportation systems.

YUNYU ZHANG received the B.E. degree in traffic and transportation from Central South University, Changsha, China. She is currently pursuing the master's degree with Beijing Jiaotong University, with a focus on the planning and management of transportation. Her research interests include transit system design, intelligent transportation systems, and connected and automated vehicles.

YINGYUE MA received the B.M. degree from Central South University, Changsha, China, where she is currently pursuing the M.E. degree. Her research interests include traffic safety, intelligent transportation systems, and reinforcement learning.